JOURNAL OF GEOPHYSICAL RESEARCH, VOL. 101, NO. D20, PAGES 25,867–25,885, NOVEMBER 20, 1996

Soil-vegetation-atmosphere processes: Simulation and field measurement for deforested sites in northern Thailand

Thomas W. Giambelluca, Liem T. Tran, Alan D. Ziegler, Trae P. Menard, and Michael A. Nullet

Climate Laboratory, Department of Geography, University of Hawaii at Manoa, Honolulu, Hawaii

Abstract. In recent efforts to predict the climatic impacts of tropical deforestation an extreme scenario of impoverished grassland has been used to represent the future deforested landscape. Currently, deforested areas of the tropics are composed of a mosaic of crops, bare soil, grassland, and secondary vegetation of various ages. The dominant feature of deforested land is often secondary vegetation. Parameter values for important forest replacement land covers, including secondary vegetation, have been shown to differ from those of forest much less than that assumed in general circulation model (GCM) deforestation experiments. For this study, the biosphere-atmosphere transfer scheme (BATS) is run in uncoupled mode using measured input data in place of GCM forcing and using the same parameter settings employed in recent deforestation experiments. Model output is compared with measurements taken over seven different deforested land surfaces in northern Thailand. Comparisons reveal that the simulation of deforested land overestimates reflected shortwave radiation, the diurnal range of surface temperature for secondary vegetation, surface soil moisture loss during periods without rain, and surface soil moisture increase at the start of a rainy period and underestimates net radiation, the diurnal range of surface temperature on recently used land surfaces, and root zone soil moisture increase at the start of a rainy period at most sites. Most deforested land surfaces, especially intermediate and advanced secondary vegetation, are more similar, in terms of land surface-atmosphere interaction, to the model simulation of forest than of deforested land as depicted in GCM experiments. These comparisons suggest that modelers aspiring to make realistic simulations of deforestation should adopt parameter settings representative of the diverse range of forest replacement land covers, instead of again using the grassland scenario.

Introduction

Explosive growth in tropical deforestation rates during the last several decades has made this an issue of critical importance. Coincident with a fivefold increase in human population during the past century, the area of human land use has increased to approximately 32% of the Earth's land surface [*Food and Agriculture Organization (FAO)*, 1990]. Within the tropics, forest land is estimated to be diminishing at an annual rate of about 14 million ha [*Myers*, 1991], with new cropland accounting for more than 10 million ha yr^{-1} [*Houghton*, 1994]. The chief concerns surrounding rapid tropical deforestation are the consequent impacts on species diversity, atmospheric chemistry, and land surface-atmosphere interaction. The latter concern has led to numerous attempts to identify possible regional and global climatic impacts of large-scale tropical deforestation on the basis of general circulation model (GCM) experiments. Investigators have attempted to simulate the effects of the shift in land surface characteristics, especially changes in radiative, aerodynamic, and soil hydraulic properties [*Wright et al.*, 1996], accompanying a shift from multistoried forest canopy to grassland. While early efforts [*Henderson-Sellers and Gornitz,* 1984] used simplistic representations of land surface processes, modelers now incorporate more realistic soil-vegetation-atmosphere transfer schemes (SVATS) into their GCMs, allowing the effects of deforestation to be represented by changes in a wide range of parameters [*Dickinson and Henderson-Sellers,* 1988]. The biosphere-atmosphere transfer scheme (BATS) [*Dickinson et al.*, 1986, 1993] has been used extensively for this purpose. Recent GCM simulations of complete tropical forest removal [*Henderson-Sellers et al.*, 1996; *McGuffie et al.*, 1995; *Sud et al.*, 1996] have shown that precipitation in the Amazon Basin and Southeast Asia would be significantly reduced as a result of lower regional evaporation and reduced moisture convergence (Table 1). Recent simulation runs predicted evaporation for the Amazon Basin would be reduced by 23 to 39% due to conversion of tropical rain forest to grassland [*Xue et al.*, 1996]. Experiments have also indicated significant changes in the atmospheric general circulation as a result of tropical deforestation, affecting the climate of regions outside the deforested areas. *Henderson-Sellers et al.* [1993a] found diminished vertical ascent in the intertropical convergence

Paper number 96JD01966.
0148-0227/96/96JD-01966$09.00

Table 1. Results of general circulation model (GCM) Deforestation Experiment [*Henderson-Sellers et al.*, 1996]; Changes in Simulated Values due to Deforestation

Instrument	Amazon	Southeast Asia
Mean maximum air temperature, K	+1.4	+0.8
Mean minimum air temperature, K	-0.3	-0.4
Mean maximum radiative surface temperature, K	+2.1	+0.8
Mean minimum radiative surface temperature, K	-1.1	-1.1
Evaporation, %	-18	-10
Rainfall, %	-21	-8

zone (ITCZ) over South and Central America and, to a lesser extent, Southeast Asia. Associated Hadley cell descent in the subtropics of both hemispheres was diminished as well.

To ascertain whether any significant regional or global climate changes due to tropical land surface change are possible, modelers have elected, in most experiments to date, to use an extreme scenario for the deforestation case, usually described as degraded pasture or impoverished grassland. In selecting grassland to represent the postforest land cover, modelers have intentionally chosen a land cover which contrasts strongly with forest in order to examine the sensitivity of the simulated coupled climate system to land cover change. As *Henderson-Sellers and Gornitz* [1984] stated in describing the first GCM deforestation experiment, the objective was to " . . . try to estimate the maximum impact likely to occur as a result of tropical deforestation by maximizing the changes important to climate." This was clearly a sound strategy at the outset of such experiments, in that were significant climatic changes not predicted under the most extreme and extensive land surface change, other less extreme scenarios would not then need to be examined. But statements by modelers such as *Polcher and Laval* [1994], who refer to the replacement of the Amazonian forest by grassland as " . . . a realistic scenario if deforestation continues at the present rate," encourage readers to forget that grassland was intentionally selected as an extreme case.

Actual land cover in tropical deforested regions is composed of a mosaic of crops, bare soil, grassland, and secondary vegetation of various ages. The cultural and economic incentives to clear forest depend on location, leading to different forest replacement covers in different regions. Cleared land in Southeast Asia is commonly used for swidden agriculture, in contrast to deforested areas of tropical America where pasture is a more common replacement. But, contrary to the perception that Amazonian forest is undergoing uniform conversion to pasture, *Moran et al.* [1994] found land in some stage of secondary succession to be the dominant feature of the Amazonian deforested areas they studied. Parameter values for a variety of forest replacement land covers in deforested areas of the eastern Amazon and northern Thailand, including secondary vegetation at various stages of development, were found to differ from those of forest much less than the settings used in previous GCM deforestation experiments [*Giambelluca*, 1996]. That study concluded that climate changes simulated for a more realistic deforestation scenario, while likely to be significant, would be less pronounced than those simulated in current deforestation experiments. *Dirmeyer and Shukla* [1994] recently demonstrated that significant precipitation decreases predicted in deforestation experiments are dependent on the magnitude of the prescribed albedo shift. Albedo changes of 0.08 are typically used in such experiments, while albedo of existing deforested areas of the Amazon and northern Thailand may only be 0.03 to 0.04 higher than forest [*Giambelluca*, 1996].

In this paper we examine land surface-atmosphere interaction for forest and deforested cases as depicted by the BATS model in comparison with measured values for seven different deforested land surfaces in northern Thailand. For this study, BATS version 1e is run in uncoupled mode using measured input data in place of GCM forcing. BATS parameter settings are those used in recent deforestation experiments. The objective of our work is to evaluate the use of parameters defined by the characteristics of impoverished grassland to represent deforested land surfaces in GCM deforestation experiments. Our intent is to compare simulated land surface-atmosphere interaction of a deforested region of the tropics as depicted in GCM experiments with that observed over seven real tropical deforested sites. Our comparisons are not intended as a critique of BATS. We have chosen not to optimize the model, as one could by using parameter settings measured for each of the field sites, but to run the model with its "default" parameters.

SVATS Validation

Improvement of parameterizations of land surface-atmosphere interaction is currently an area of active research including efforts such as the Project for Intercomparison of Land-Surface Parameterization Schemes [*Henderson-Sellers and Dickinson*, 1992; *Pitman et al.*, 1993; *Henderson-Sellers et al.*, 1993b, 1995; *Love and Henderson-Sellers*, 1994; *Henderson-Sellers*, 1995; *Pitman and Henderson-Sellers*, 1995] which is aimed at comparing results of different SVATS. On the basis of these intercomparisons, *Henderson-Sellers et al.* [1995] strongly recommend further testing of SVATS. Comparison of simulations with observed energy fluxes and land surface state variables such as surface temperature and soil moisture offer the best means of testing and improving existing models. Much has been learned about parameterizations of surface-atmosphere mass and energy exchange in SVATS through large-scale field measurement programs such as Amazon Region Micrometeorological Experiment (ARME) [*Shuttleworth et al.*, 1984a, b; 1991]; Hydrologic Atmospheric Pilot Experiment - Modelisation du Bilan Hydrique (HAPEX-MOBILHY) [*Andre et al.*, 1986], First ISLCP Field Experiment (FIFE) [*Sellers et al.*, 1988], and Anglo-Brazilian Amazonian Climate Observation Study (ABRACOS) [*Wright et al.*, 1992, 1996; *Culf et al.*, 1995; *Xue et al.*, 1996]. The data sets from these programs serve as input to force SVATS and output against which SVATS-simulated values can be validated [e.g., *Noilhan and Planton*, 1989; *Mahfouf and Jacquemin*, 1989; *Mahfouf*, 1990; *Jacquemin and Noilhan*; 1990; *Betts et al.*, 1993, 1996; *Chen et al.* 1996]. In addition, measurements taken

Table 2. Biosphere-atmosphere-transfer-scheme (BATS) version 1e Vegetation/Land Cover Parameters for Evergreen Broadleaf Trees and Tall Grass [*Dickinson et al.*, 1993]

Parameter	Type 6, Evergreen Broadleaf Trees	Type 7, Tall Grass
Maximum fractional vegetation cover	0.90	0.80
Maximum fractional vegetation cover minus cover at 269 K	0.5	0.3
Vegetation roughness length, m	2.0	0.1
Depth of the rooting zone soil layer, m	1.5	1.0
Depth of the upper soil layer, m	0.1	0.1
Fraction of water extracted by upper layer roots (saturated)	0.8	0.8
Vegetation albedo < 0.7 μm	0.04	0.08
Vegetation albedo > 0.7 μm	0.2	0.3
Minimum stomatal resistance, s m^{-1}	150	200
Maximum leaf area index	6.0	6.0
Minimum leaf area index	5.0	0.5
Stem and dead matter area index	2.0	2.0
Inverse square root of leaf dim., $m^{-1/2}$	5	5
Light sensitivity factor (m^2 W^{-1})	0.06	0.02

in smaller-scale field measurement projects over various land covers have been used to test SVATS simulations, including those of the simple biosphere (SiB) model [Sellers et al., 1986, 1989; Sellers and Dorman, 1987] and BATS [Shuttleworth, 1988; Dickinson, 1989; Dickinson and Henderson-Sellers, 1988].

Biosphere-Atmosphere Transfer Scheme (BATS)

BATS is a comprehensive model of landsurface processes for climate and climate models with emphasis on the proper description of the role of vegetation in modifying the surface moisture and energy budgets. BATS was initially used primarily as the land surface interface for the community climate model (CCM) of the National Center for Atmospheric Research [*Dickinson et al.*, 1986, 1993] but has since been used widely for a variety of on-line and off-line applications. As in other SVATS, the primary functions of BATS are determination of the fraction of incident solar radiation absorbed by different surfaces and their net exchange of thermal infrared radiation; calculation of transfers of momentum, sensible heat, and moisture between the Earth's surface and the atmosphere; determination of wind, humidity, and temperature of the atmosphere within canopies and at surface reference level; and determination of temperature and moisture quantities at the Earth's surface, including soil moisture content of different soil layers and runoff from excess rainfall. When BATS is coupled with the CCM, parameter settings are assigned to terrestrial areas on the basis of the categorization of each grid square as one of 18 vegetation/land cover types, 12 soil texture classes, and eight soil color classes.

In simulating the climatic effects of tropical deforestation, BATS has been used several times with the CCM [*Dickinson and Kennedy*, 1992; *Henderson-Sellers et al.*, 1993a, 1996]. In these experiments, control runs are made with tropical forest areas represented by vegetation/land cover parameters set for evergreen broadleaf trees and soil parameters based on representative soil texture and color classes. Results of the control run are compared with those of an experimental run in which tropical forest areas are assigned land cover parameters for tall grass and in which soil parameters are shifted to a finer texture class and a lighter color class. Table 2 lists parameter settings for evergreen broadleaf trees and tall grass as given by *Dickinson et al.* [1993] for use with BATS version 1e. Table 3 gives the BATS version 1e parameter settings for the two soil texture classes used in recent deforestation experiments. Table 4 gives those for soil color classes.

Table 3. BATS Version 1e Soil Parameter Settings for Soil Texture Classes Used in Recent Deforestation Experiments [*Dickinson et al.*, 1993]

Parameter	Class 10, forest	Class 12, deforested
Porosity	0.60	0.66
Minimum soil suction, mm	200	200
Saturated hydraulic conductivity, mm s^{-1}	0.0016	0.0008
Ratio of saturated thermal conductivity to that of loam	0.80	0.70
Exponent "B" defined in *Clapp and Hornberger* [1978]	9.2	10.8
Moisture cont. relative to saturation at which transpiration ceases	0.487	0.542

Methods

Research Strategy

BATS can be operated uncoupled from its parent GCM by providing the time-dependent atmospheric forcing variables. In this study, BATS was used to simulate land surface-atmosphere interaction over a deforested region in northern Thailand. Measured downward shortwave radiation, rainfall, air temperature, humidity, and wind speed served as forcing for the model in uncoupled mode. Two model runs, using parameter settings for forest and deforested cases, were made using the same input data set. Selected model output from each of the two runs, namely, reflected shortwave radiation, canopy temperature, net radiation, soil moisture in the upper 10 cm, and root-zone soil moisture, were compared with field measurements of those variables at a variety of different deforested sites. These comparisons allow us to evaluate the extent to which land surface-atmosphere interaction, especially canopy radiative

Table 4. BATS Version 1e Soil Parameter Settings for Soil Color Classes Used in Recent Deforestation Experiments [*Dickinson et al.*, 1993]

Parameter	Class 4, forest	Class 2, deforested
Dry soil albedo < 0.7 μm	0.18	0.22
Dry soil albedo > 0.7 μm	0.36	0.44
Saturated soil albedo < 0.7 μm	0.09	0.11
Saturated soil albedo > 0.7 μm	0.18	0.22

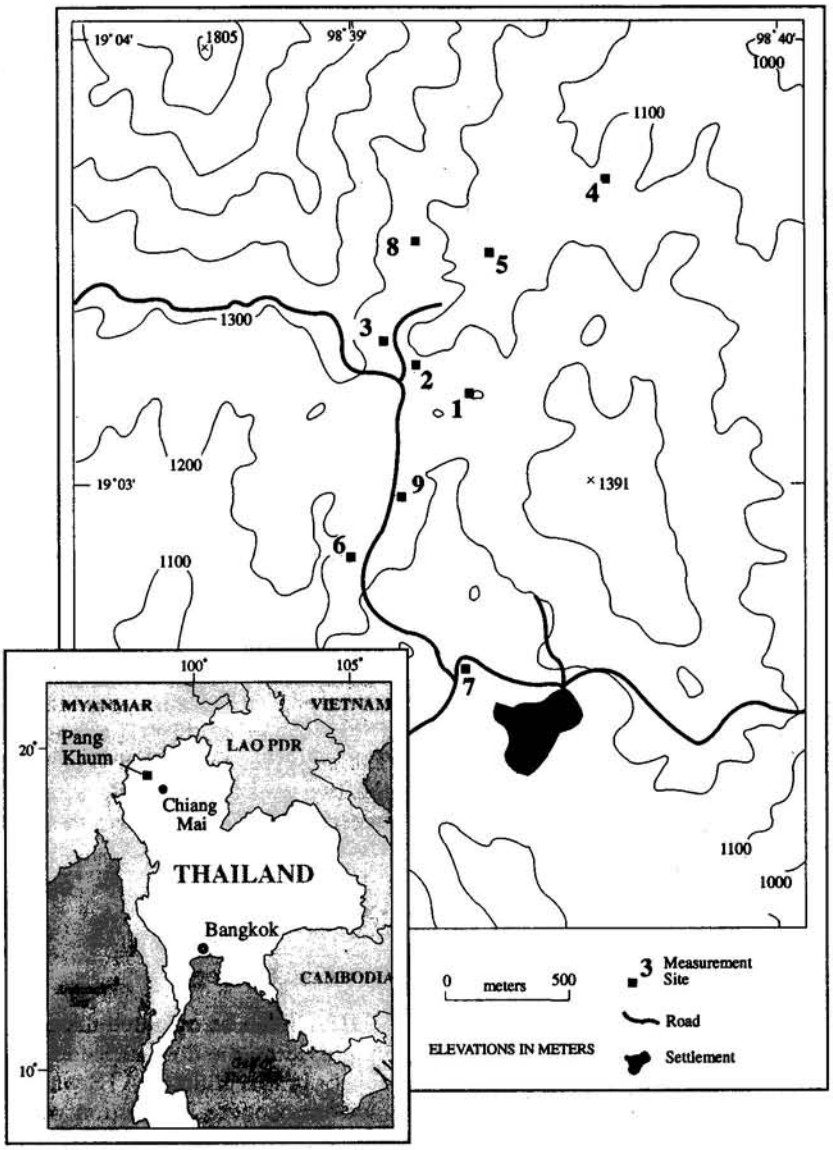

Figure 1. Study site locations, Pang Khum, Thailand.

exchange and soil moisture change, simulated in GCM experiments of future deforestation resembles that measured over real present-day tropical deforested sites.

Land cover change alters fluxes of energy and mass and results in mutual adjustments of the states of the surface and the atmosphere. Use of a single measured data set to force BATS in an off-line mode for simulations under two different parameter settings does not allow atmosphere-land surface feedbacks that would be present in reality. The existence of these feedbacks is an important reason why coupled GCM-SVATS must be used to predict the effects of tropical deforestation.

Study Area

Field data for the model simulation were collected during January through May 1993 in Chiang Mai Province, northern Thailand, an area of active deforestation. Measurements were made near the village of Pang Khum located at an altitude of 1250 m in the mountainous region north of the city of Chiang Mai (Figure 1). Pang Khum was originally settled 200 years ago by the ethnic hilltribe group known as the Karen. During the past 20 years a group of Lisu people has joined the Karen residents of the village. The villagers of both groups practice swidden agriculture on the slopes surrounding the settlement [*Fox et al.*, 1994]. Paddy rice is also grown on terraced fields in the valley bottoms. While in the past, agriculture consisting of swidden crops was chiefly for subsistence, now vegetables, fruit, barley, and cut flowers are also grown for sale outside the village. Because of government- and international aid agency-sponsored incentives as well as police enforcement, the once prevalent opium poppy is now grown only in a few small plots. Natural vegetation in the region can be described as lower montane forest. *Richards and Flint* [1994] show that extensive forest loss in northern Thailand during the 100 years ending in 1980 was coincident with expansion of cultivated land and grass/shrub land. In a study of vegetation in an area with similar terrain about 70 km ENE of Pang Khum, *Hansen* [1992] declared that no undisturbed primary forest remains. This is probably also true of the Pang Khum area, although stands of mature old growth and exploited primary forest are in evidence. The population of

Table 5. Characteristics of Measurement Sites at Pang Khum, Chiang Mai Province, Northern Thailand; Measurement Period for Meteorological and Soil Moisture Measurements

Map Code[a]	Land Cover	Elevation (m)	Slope[b] (degree)	Aspect[b] (degree)	Vegetation Height[c] (m)	Meteorological Data Start	Meteorological Data End	Soil Moisture Content Start	Soil Moisture Content End
1	Secondary vegetation (8 year)	1290	21	300	3.2	Jan. 24	March 7	Jan 17	May 27
2	Secondary vegetation (2 year)	1220	18	35	1.9	March 7	March 13	March 9	May 27
3	Harvested barley	1240	17	65	0.3	March 13	March 21	-	-
4	Irrigated exposed soil	1120	9	270	0.0	March 24	March 30	-	-
5	Secondary vegetation (3 year)	1170	3	75	1.7	March 30	April 8	-	-
6	Secondary vegetation (25 year)	1240	14	310	5.6	April 9 (and)	April 21 May 11 May 24	April 9	May 27
7	Fallow rice paddy	1120	0	--	0.0	April 26	May 11	-	-
8	Harvested corn	1245	10	87	0.2	-	-	Jan. 17	May 27
9	Exploited primary forest	1245	5	270	25.0	-	-	Feb. 2	May 27

[a] Refer to site numbers shown in Figure 1.

[b] Slope and aspect pertain to a spatial scale of approximately 100 m.

[c] Mean vegetation height.

the village as well as the surrounding region is growing rapidly [*Fox et al.*, 1995]. The increased land pressure has reduced fallow periods and expanded the area of cultivation at the expense of old growth forest. The climate of the region is monsoonal, with a well-defined annual rainfall cycle. The rainy season extends from mid-May through October or early November, during which approximately 90% annual rainfall occurs. Mean annual rainfall in the area is approximately 1000-1200 mm, although data from recorded at Doi Mon Ang Get (1300 m elevation), a station close to Pang Khum, averaged about 3000 mm over a six year period, suggesting that at least some areas receive greater amounts of rainfall due to orographic effects. Mid-November through late February is the cool season with mean air temperatures of around 17°C. During the hot season, March to mid-May, air temperature averages about 25°C, reaching daytime highs above 30°C.

Field Data

Meteorological measurements were taken in Pang Khum using a single set of sensors which were moved from site to site to produce a sequence of observations for seven different land covers. During the course of field work, five soil moisture measurement stations were established, three of which are located at meteorological measurement sites. Meteorological and soil moisture measurement sites are described in Table 5; locations are shown in Figure 1. "Exploited primary forest" refers to an area where large old growth trees remain but where canopy, understory, and soil characteristics have been affected by limited wood harvesting and the presence of livestock. Meteorological and soil field instruments and data recording equipment are listed in Table 6. Meteorological measurements were sampled at a 5-s interval with 10-min means recorded at all sites except site 1, where hourly means were logged. Measurement results are described in detail by *Giambelluca* [1996]. Soil moisture measurements were made for five or more depth ranges at each of the five sites using a time-domain reflectometry (TDR) device [cf. *Dalton*, 1992]. Soil probes were installed and remained in place throughout the measurement period at each site. Soil moisture readings were generally taken on a weekly interval. Canopy and soil parameters derived from data measured at each site are given in Table 7 [*Giambelluca*, 1996].

Data Set Preparation

Sequentially measured data sets from the seven study sites at Pang Khum covered the period from January 24 to May 23, 1993. Our strategy called for developing a continuous input data set to force BATS for the entire period, consisting of 19,679 10-min intervals. To do so, we combined measurements taken at the different sites, adjusted

Table 6. Sensors and Data Recorders

Instrument	Company	Location	Model
Shortwave radiation			
downward	Eppley Laboratory	Newport, R.I.	8-48
reflected	Eppley Laboratory	Newport, R.I.	PSP
Net all-wave radiation	REBS	Seattle, Wash.	Q*6
Canopy temperature	Everest Interscience	Fullerton, Calif.	4000ALCS
Air temperature and humidity	Vaisala	Helsinki, Finland	HMD30UYB
Wind velocity	R.M. Young	Traverse City, Mi.	27005UVX
Rainfall rate	Campbell Sceintific	Logan, Utah	TE525
Soil water content	Soilmoisture Equipment	Santa Barbara, Calif.	6050X1 Trase System 1
Soil hydraulic conductivity	Franklin Precision Eng.	Brookvale, Australia	CSIRO disk permeameter
Data loggers	Licor	Lincoln, Neb.	LI-1000

Table 7. Canopy and Soil Characteristics of Meteorological Measurement Sites, Pang Khum Thailand [*Giambelluca*, 1996]

Site	α[a]	d[b]	z[c]	K_s[d]	Representative Species[e]
1	0.115	2.16	0.41	3.3×10^{-5}	*Lithocarpus elegans* (Bl.) Hatus. ex Soep. (Fagaceae) *Gluta tavoyana* Wall. ex Hk. f. (Anacardiaceae)
2	0.134	1.32	0.25	1.1×10^{-4}	*Ageratina adenophorum* (Spreng.) R. King and H. Robinson (Compositae) *Coffea arabica* L. var. arabica (Rubiaceae)
3	0.163	0.00	0.04	5.4×10^{-5}	no live vegetation
4	0.085	0.09	0.02	1.2×10^{-4}	no live vegetation
5	0.171	1.21	0.23	8.4×10^{-6}	*Imperata cylindrica* (L.) P. Beauv. var. *major* (Nees) C.E. Hubb. ex Hubb. & Vaugh. (Gramineae) *Thysanolaena latifolia* (Roxb. ex Horn.) Honda (Gramineae)
6	0.135	3.80	0.73	2.9×10^{-4}	*Lithocarpus elegans* (Bl.) Hatus. ex Soep. (Fagaceae) *Gluta tavoyana* Wall. ex Hk. f. (Anacardiaceae)
7	0.141	0.01	0.001	2.5×10^{-5}	*Fimbristylis aestivalis* (Retz.) Vahl. var. *aestivalis* (Cyperaceae) *Digitaria seigera* Roth ex Roem. & Schult. var. *setigera* (Gramineae)

[a]Shortwave albedo (ratio)
[b]Zero plane displacement height, m.
[c]Roughness length, m.
[d]Soil saturated hydraulic conductivity, m s^{-1}.
[e]Vegetation taxonomy by F. Maxwell, Biology Department, Chiang Mai University.

height-sensitive measurements to a comparable reference level, and employed several techniques to fill gaps in the measurement record resulting from moving instruments between sites and temporary instrument failures.

Air temperature, humidity, and wind measurements, recorded at two or three heights above the canopy at each site, were standardized to a reference level 5 m above the zero plane displacement height (Table 7) by interpolating or extrapolating linearly from the two nearest sensors (Table 8).

Wind data at all sites were adjusted to the reference height using the following relationship:

$$U_{5.0} = U_z \frac{\ln(5.0+d) - \ln(z_0)}{\ln(z+d) - \ln(z_0)} \quad (1)$$

where $U_{5.0}$ is the wind speed adjusted to the reference level of 5 m above the zero plane displacement height; U_z is the measured wind speed; z is the measurement height; d is the zero plane displacement height; and z_0 is the roughness length. The parameters d and z_0 (Table 7) were estimated previously using wind profile measurements at each site [*Giambelluca*, 1996].

Rainfall was estimated from under-canopy rainfall collection to total approximately 50 mm for the period May 11-18, during which the rain gage was rendered inoperative by an infestation of ants. Six storm sequences totaling 53 mm taken from the adjacent record were substituted into the data gap at times when net radiation and relative humidity suggested rainfall.

Ten-minute data were interpolated from hourly data at site 1. Missing values within data gaps longer than 3 hours were computed as the mean of values recorded at the same time of day during the preceding and following one to two

Table 8. Heights of Sensors and Reference Level at Each Site

Site	Period	z_u[a]	$z_{(T/RH)_1}$[b]	$z_{(T/RH)_2}$[b]	$z_{(T/RH)_3}$[b]	$z_{5.0}$[c]
1	Jan. 24-30	7.56	5.56	7.56	-	7.16
	Jan. 30 to March 2	10.32	7.45	9.90	-	7.16
	March 4-7	10.32	1.40	9.90	-	7.16
2	March 7-13	6.50	3.77	6.04	-	6.32
3	March 13-24	5.21	2.48	4.75	-	5.00
4	March 24-30	5.20	0.70	2.35	4.75	5.09
5	March 30 to April 8	6.99	2.44	4.06	6.57	6.21
6	April 9-21; May 11-24	11.90	9.82	11.45	13.95	8.80
	April 21-25	11.90	9.82	2.00	13.95	8.80
7	April 26 to May 11	4.62	0.70	2.17	4.22	5.01

[a] Height of wind sensor.
[b] Heights of the temperature/humdity sensors.
[c] Reference height to which wind, temperature, and humidity measurements were adjusted.

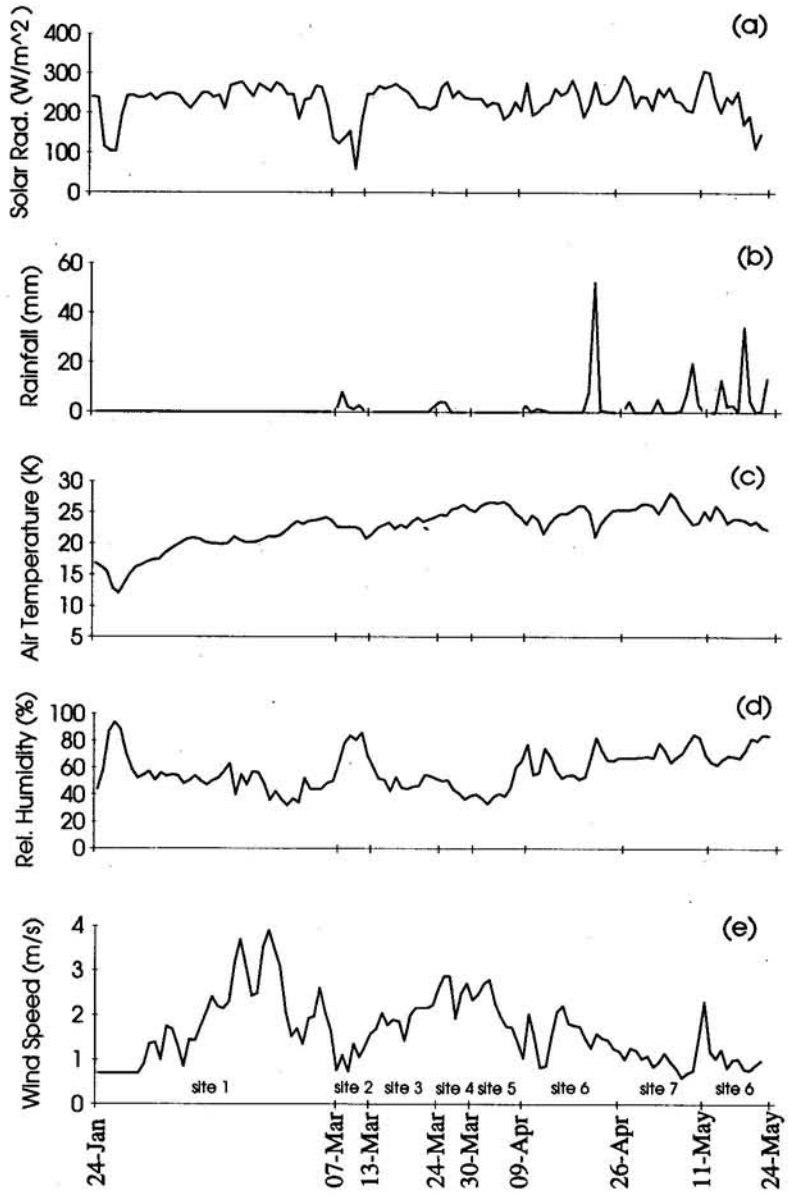

Figure 2. Daily means of (a) solar radiation, (b) rainfall, (c) air temperature, (d) relative humidity, (e) and wind speed derived from measurements at Pang Khum, Thailand, January 24 to May 23, 1993.

days. Values for gaps smaller than 3 hours were interpolated linearly from the values immediately before and after the gap. Missing downward shortwave radiation for sites 1, 2, 6, and 7 were filled using linear regression equations relating solar and net radiation based on concurrent measurements at each site. Coefficients of determination (r^2) were all greater than 0.99.

The daily means from the 10-min data set for solar radiation, rainfall, air temperature, humidity, and wind speed are shown in Figure 2. Periods of observation corresponding to each of the seven meteorological measurement sites are shown along the time axis. Estimation, interpolation, and extrapolation of values to fill periods when measurements were missing was done only for the purpose of allowing a continuous model simulation run. In direct comparisons among model output and measured data that follow, we will exclude all periods without a complete measured input data set.

Figure 2 demonstrates that climatic conditions varied significantly during the observations that spanned the period from the end of the "cold" (and dry) season in late January and early February through the "hot" (and dry) season of March and April into the beginning of the rainy season in May. We should emphasize here that measurements at different sites were not made simulateously. Therefore direct comparisons among sites are not possible because of the changing ambient condtions.

Model Runs

In the off-line version of BATS, diffuse shortwave radiation is approximated as a constant fraction of solar radiation. We modified the code to estimate the diffuse component using the empirical relationship determined by *Erbs et al.* [1982]:

Table 9. BATS Initial Conditions and Parameter Settings for Forest and Deforested Runs

Variable	Forest	Deforested
Fractional vegetation cover	0.90	0.80
Landcover/vegetation category	6	7
Starting root zone soil moisture, mm	570.	484.
Starting total soil moisture, mm	3821.	4924.
Starting upper soil moisture, mm	34.	45.
Soil texture category	10	12
Soil color category	4	2
Time step (second)	600	600

$$\frac{Id}{I} = \begin{cases} 1.0 - 0.09Mt & 0.0 \le Mt \le 0.22 \\ 0.9511 - 0.1604Mt + 4.388Mt^2 & \\ \quad -16.638Mt^3 - 12.336Mt^4 & 0.22 < Mt \le 0.80 \\ 0.165 & 0.80 < Mt \end{cases} \quad (2)$$

where I_d is hourly diffuse radiation, I is hourly solar radiation, $M_t = I/I_0$, and I_0 is hourly extraterrestrial solar radiation on a horizontal surface.

Settings for forest and deforested runs are those used in recent GCM deforestation experiments (Table 9). Starting soil moisture content values are based on field measurements.

Model Output

Figure 3 summarizes selected BATS output variables for the forest and deforested runs using the Pang Khum data set. Shown are daily time series of reflected shortwave radiation, minimum and maximum surface temperature, net radiation, surface soil moisture change, root zone soil moisture change, evaporation, and sensible heat flux. Table 10 gives a statistical summary of the model output for the two runs. As expected, reflected shortwave radiation (Figure 3a) closely resembles the course of daily solar radiation (Figure 2a) with much higher amounts reflected by the simulated deforested surface (40 W m^{-2} on average) than the simulated forest (26 W m^{-2}). Despite having more than 50% greater reflected radiation, the simulated deforested surface had daily maximum surface temperatures (Figure 3b) more than 7 K higher than the simulated forest. The model predicts lower daily surface temperature minima after deforestation, so that the overall mean is about 1.4 K lower due to deforestation, while the diurnal range is greatly increased. Greater shortwave reflection and higher daytime surface temperature result in lower net radiation (Figure 3c) for the deforested run as compared with the forest.

Soil moisture for the surface layer (Figure 3d) and the root zone (Figure 3e) is given in terms of the change from the start of the simulation. From the beginning of the simulation to the third week of April, the Southeast Asian winter

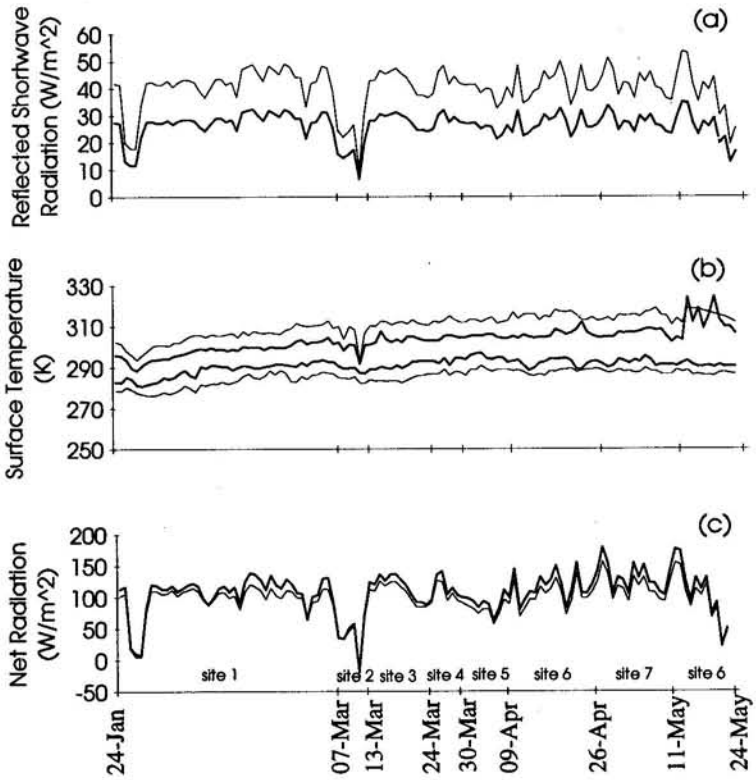

Figure 3. Biosphere-atmosphere-transfer-scheme (BATS) model output summary forest (thick lines) and deforested (thin lines) runs for Pang Khum, Thailand: (a) daily means of simulated reflected shortwave radiation; (b) daily minima and maxima of simulated surface temperature; (c) daily means of simulated net radiation; (d) change in daily means of soil moisture content in the upper 0.1-m layer; (e) change in daily means of simulated soil moisture content in the root zone (forest, upper 1.5-m layer; deforested, upper 1-m layer; (f) daily means of simulated evaporation; and (g) daily means of simulated sensible heat flux in Pang Khum, Thailand, January 24 to May 23, 1993.

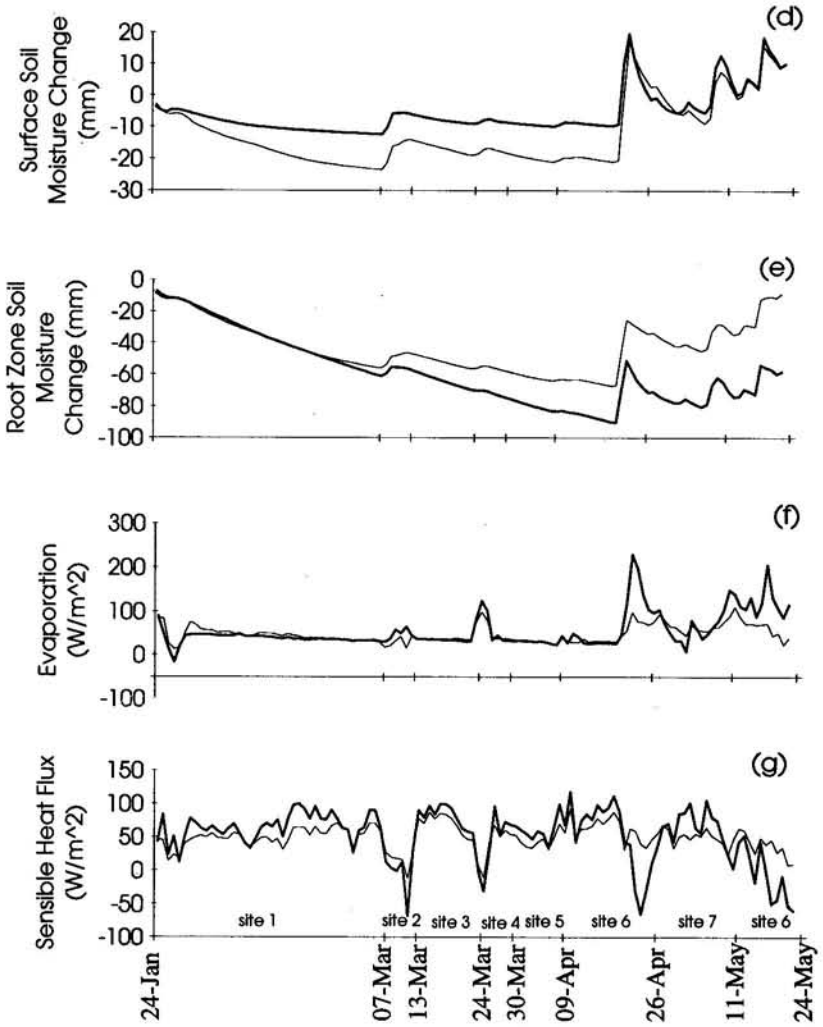

Figure 3. (continued)

monsoon prevailed, and the dry season was interrupted only briefly during the second week of March. Surface soil moisture during that period dropped more rapidly in the deforested case because the reduced vegetative cover in the simulation produces higher direct soil evaporation. In comparing root zone soil moisture change, note that root depth is set at 1.5 m for forest and 1.0 m for the deforested case. Dry season reduction of root zone soil moisture is greater for the forest primarily because of the greater root depth and hence larger soil moisture reservoir available to the forest. After the rains begin, surface soil moisture for the two runs are very similar, while root zone moisture increases more rapidly for the deforested case. Evaporation rates (Figure 3f) are remarkably similar for the two cases throughout the dry season and differ significantly only after the rain begins. A comparison of the evaporation rates for the rainy period suggests that the slower root zone soil moisture gains for forest seen in Figure 3e are due to higher rates of evaporation (more intercepted water and lower canopy resistance to transpiration). During most of the dry season, sensible heat flux (Figure 3g) is greater for forest than for the deforested case, despite lower daytime surface temperature. Presumably this is due to the relatively higher nighttime temperature and greater roughness length for the forest. During the rainy period, forest sensible heat flux is highly variable in comparison with the deforested case.

Comparison of Simulations With Observations

Comparisons of simulated and observed reflected shortwave radiation, surface temperature, and net radiation are given graphically for 2-day sample periods at each measurement site in Figures 4-6, and in terms of period-of-measurement summary statistics in Table 11. Root-mean-square-error (RMSE) computed from differences between observed and simulated values for each model run are given in Table 12. In Figures 4-6, sites are arranged from most disturbed (bare soil) to least disturbed (25-year secondary vegetation), rather than chronologically. For site 6 (25-year secondary vegetation), two 2-day periods are shown, before (g) and after (h) the start of the rainy season. Simulated and observed surface and root zone soil moisture change are shown for the entire measurement period at each TDR site in Figures 7 and 8. Again, direct comparisons among sites are not possible because measurements were not made simultaneously and differ because of varying ambient conditions.

Table 10. Statistics of BATS-Estimated Outputs (Reflected Shortwave Radiation, Surface Temperature, Net Radiation, Surface Soil Moisture Change, Root Zone Soil Moisture Change, Evaporation, and Sensible Heat flux) for Forested and Deforested Cases for Pang Khum, Thailand, During January 24 to May 23, 1993

Climate Variable	Case	Mean	Mean Daily Minimum	Mean Daily Maximum	Standard Deviation
Reflected shortwave radiation, W m^{-2}	Forested	26.3	0.0	107.7	36.5
	Deforested	40.1	0.0	164.4	55.7
Surface temperature, K	Forested	295.4	290.6	303.1	4.9
	Deforested	294.0	285.3	310.3	8.8
Net radiation, W m^{-2}	Forested	107.1	-96.3	713.0	268.9
	Deforested	96.8	-74.7	615.4	225.9
Surface soil moisture change, mm	Forested	-5.4	-6.3	-4.5	7.1
	Deforested	-11.8	-12.7	-10.9	10.4
Root zone soil moisture change, mm	Forested	-55.0	-56.3	-53.8	21.6
	Deforested	-39.6	-40.6	-38.6	16.5
Evaporation, W m^{-2}	Forested	55.2	-42.1	395.1	111.4
	Deforested	47.5	-1.6	200.7	66.0
Sensible heat flux, W m^{-2}	Forest	52.1	-234.0	596.6	222.0
	Deforested	49.3	-64.3	389.9	134.8

In accordance with the site albedo values given in Table 7, measured reflected shortwave radiation is lower at every site than simulated for the deforested case (Table 11 and Figure 4). On the basis of RMSE (Table 12), measured reflection is more similar to the model forest than to the model deforested surface except at the two sites with the highest albedo, sites 3 (harvested barley; albedo, 0.163) and 5 (3-year secondary vegetation; albedo, 0.171). At site 4 (bare soil; albedo, 0.085), observed reflection is low because the soil was kept wet and thus dark by irrigation during the measurement period. The effect of irrigation on albedo of the bare soil is particularly noticeable near the beginning of the 2-day sample period, which follows an irrigation round, and near midday on the second day when reflection drops abruptly in response to another round of irrigation. Reflection for agricultural and young secondary vegetation surfaces (sites 2, 3, 5, and 7) generally lies between those of the two simulations. For 8- and 25-year secondary vegetation (sites 1 and 6; albedo, 0.115 and 0.135, respectively), observed reflected shortwave radiation is very similar to that of the model forest.

In general, the divergence from observations of simulated shortwave reflection for the deforested run stems from the use of an excessively large albedo shift. As mentioned earlier, the observations reported for this study area and for a deforested area of the eastern Amazon suggest an upward albedo shift of 0.03 to 0.04 rather than the 0.08 commonly used to represent the effects of deforestation [*Giambelluca*, 1996].

Surface temperature estimated by the model is derived from estimated leaf and soil surface temperatures, weighted on the basis of the fractional vegetation coverage (Table 2). Because leaf temperature involves radiative and turbulent canopy-ground and canopy-atmosphere energy exchange processes, surface temperature is a very useful diagnostic variable for assessing model performance. As was evident in Figure 3b and Table 10, modeled surface temperature for the deforested simulation has a similar mean but a significantly higher-amplitude diurnal cycle than that of the forest simulation (Figure 5). During the 2-day sample (Figure 5), bare soil observations are reasonably close to the deforested simulation except when the soil surface was wet from irrigation during the early daylight hours of the first day and the afternoon of the second day. In the mean (Table 11), measured surface temperature at the bare soil site was lower than either simulation and thus closer to the deforested run than to the forest simulation. Mean measured values were higher than either simulation for the fallow rice paddy and the 3-year secondary vegetation sites and between the two simulations for the 2-year secondary vegetation (site 2). For the harvested barley surface (site 3), where a very dry soil surface was almost fully exposed, extremely high daytime surface temperatures were observed, exceeding those of the deforested simulation by nearly 12 K. Surface temperature of the fallow rice paddy (site 7) and 3-year secondary vegetation (site 5) resembled that of the simulated deforested surface during the day and the simulated forest at night. The diurnal range of measured surface temperature was greater than either simulation for the bare soil and harvested barley sites; between the two simulations for the fallow rice paddy, and 2-year, 3-year, and 8-year secondary vegetation sites; and lower than either simulation for the 25-year secondary vegetation site. For the 2-year secondary vegetation (site 2), which experienced a significant premonsoon rainfall during its observation period, and for 8-year and 25-year secondary vegetation (sites 1 and 6), measured surface temperature appears to be very well depicted by the forest simulation (Figure 5). Surface temperature RMSEs for observed versus modeled forest at those three sites are between 1.29 and 1.62 K, lowest of the forest simulations and lower than all sites for the deforested simulation (Table 12). Surface temperature for harvested barley, exposed soil, and 3-year secondary vegetation (sites 3, 4, and 5) had lower RMSEs

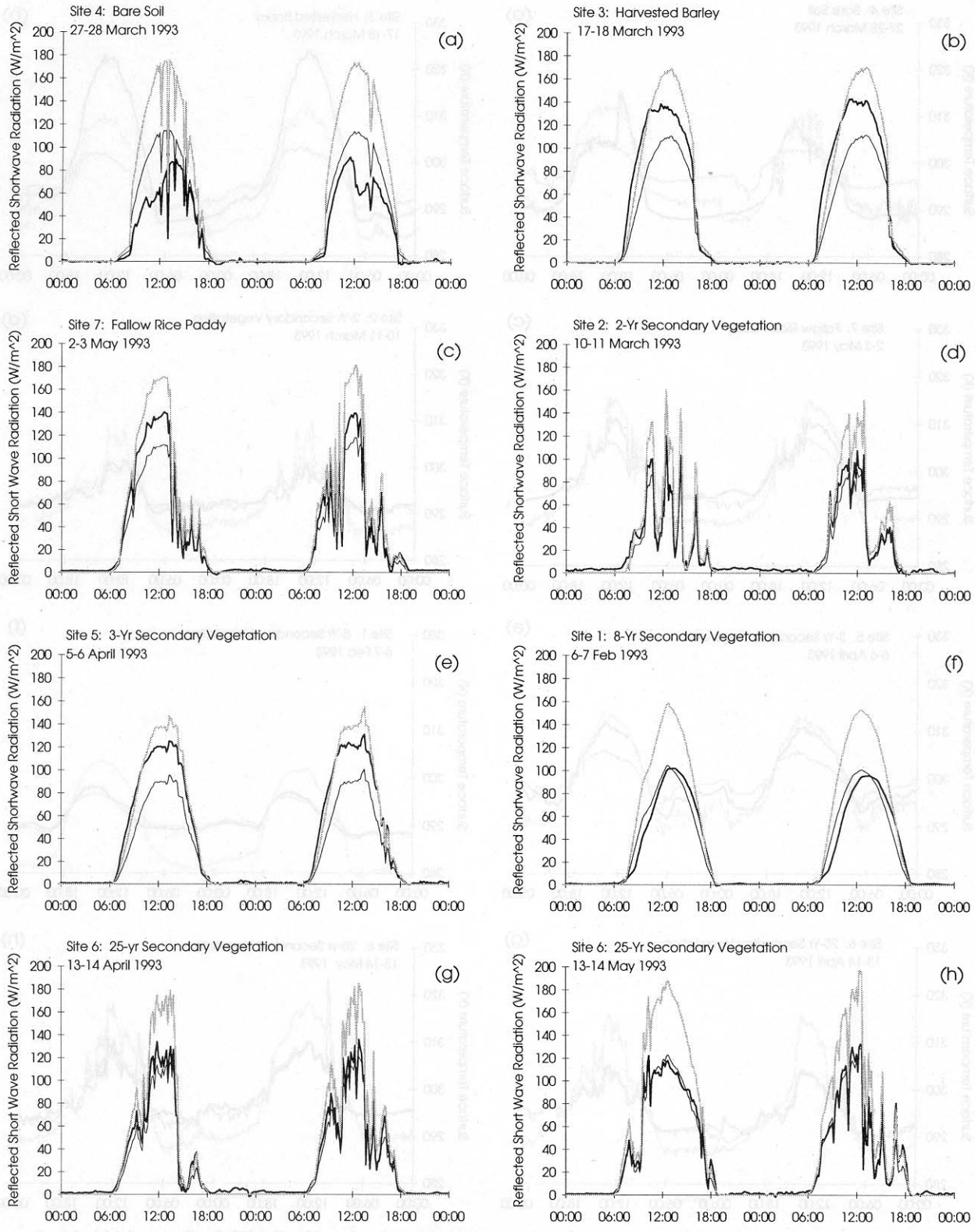

Figure 4. Representative 2-day samples of reflected shortwave radiation simulated by BATS for forested (thin black line) and deforested (grey line) sites and measured (thick black line) over (a) irrigated bare soil, (b) harvested barley, (c) fallow rice paddy, (d) 2-year secondary vegetation, (e) 3-year secondary vegetation, (f) 8-year secondary vegetation, (g) 25-year secondary vegetation before rainy period, and (h) 25-year secondary vegetation during rainy period.

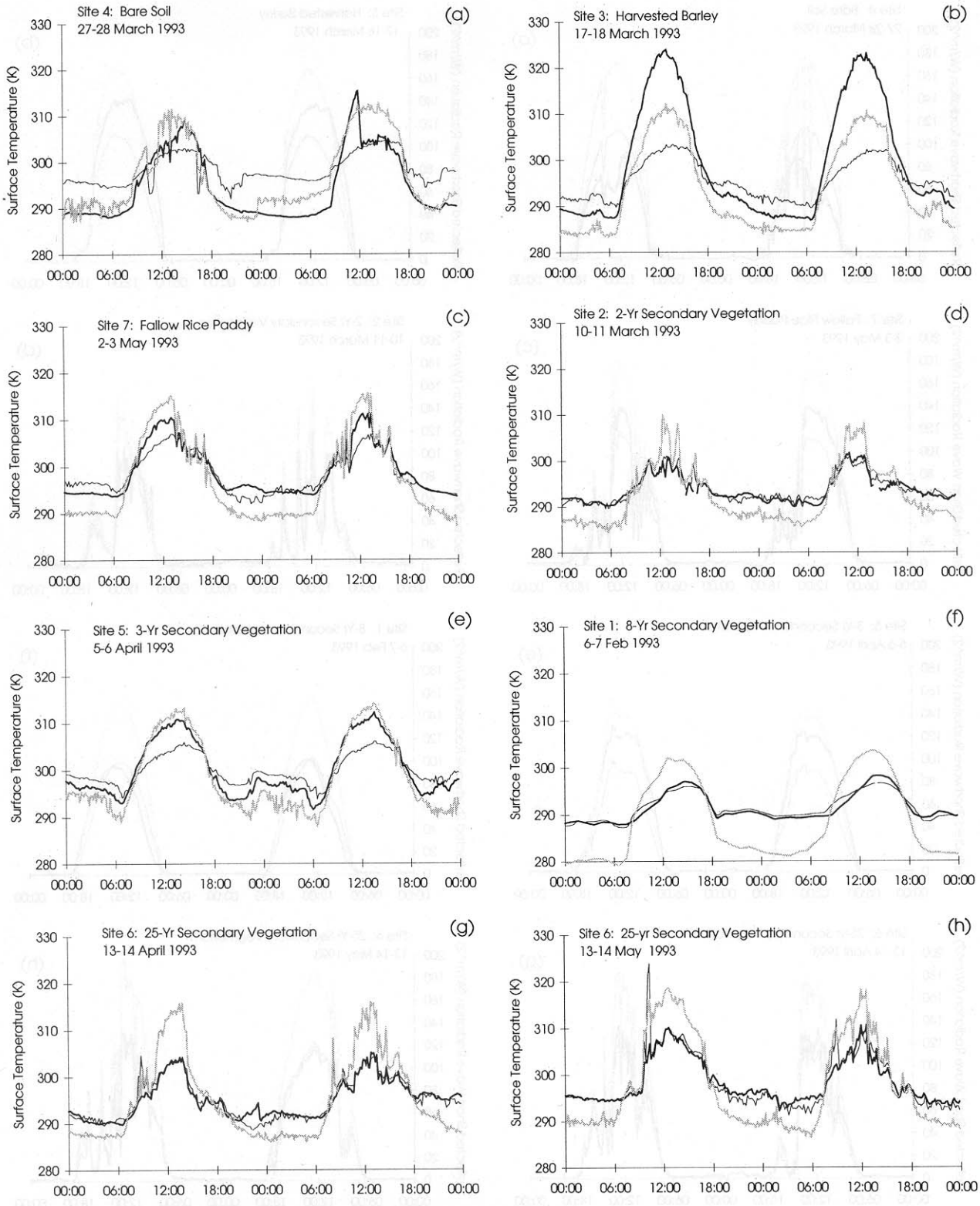

Figure 5. Representative 2-day samples of surface temperature simulated by BATS for forested (thin black line) and deforested (grey line) sites and measured (thick black line) over (a) irrigated bare soil, (b) harvested barley, (c) fallow rice paddy, (d) 2-year secondary vegetation, (e) 3-year secondary vegetation, (f) 8-year secondary vegetation, (g) 25-year secondary vegetation before rainy period, and (h) 25-year secondary vegetation during rainy period.

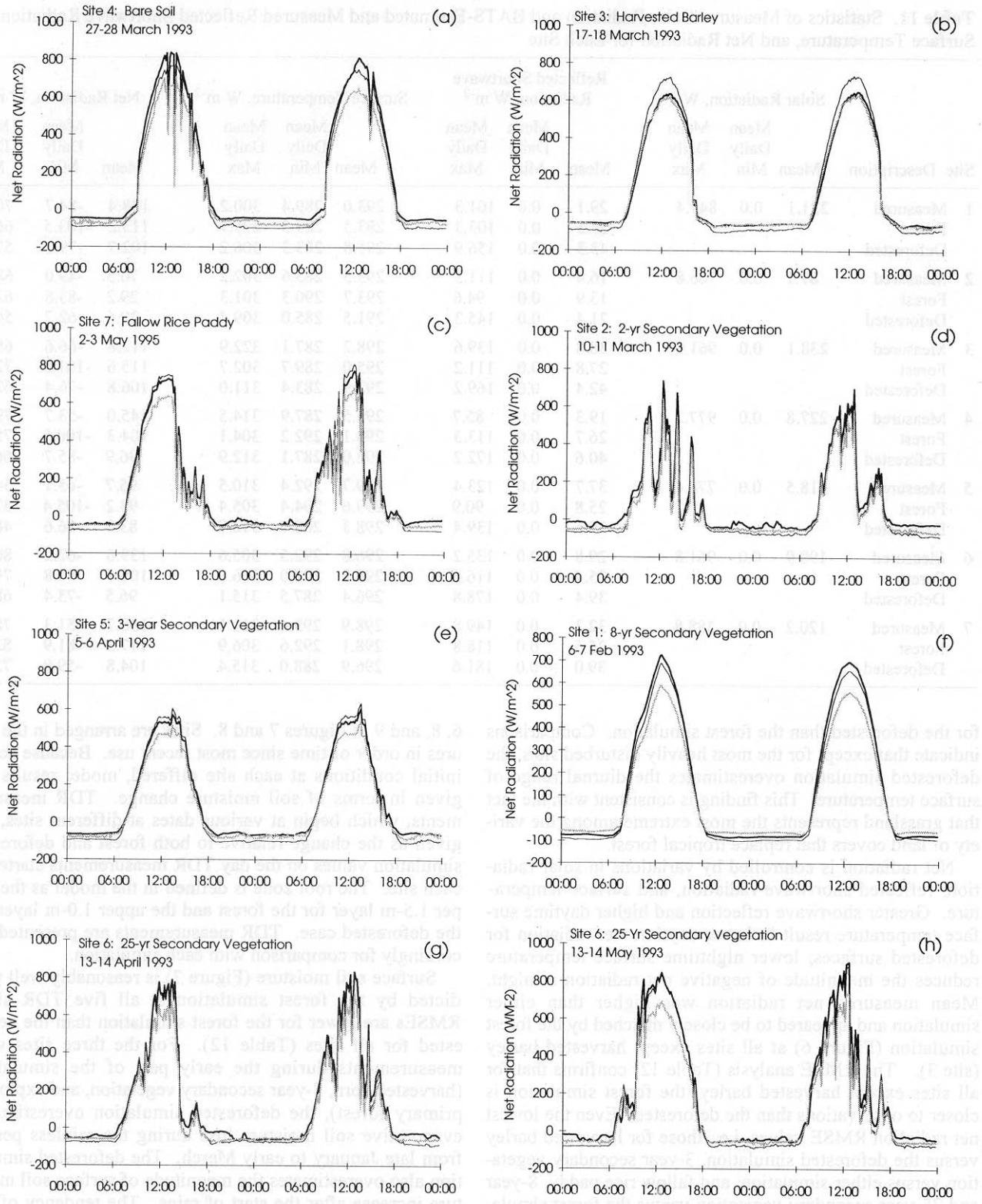

Figure 6. Representative 2-day samples of net radiation simulated by BATS for forested (thin black line) and deforested (grey line) sites and measured (thick black line) over (a) irrigated bare soil, (b) harvested barley, (c) fallow rice paddy, (d) 2-year secondary vegetation, (e) 3-year secondary vegetation, (f) 8-year secondary vegetation, (g) 25-year secondary vegetation before rainy period, and (h) 25-year secondary vegetation during rainy period.

Table 11. Statistics of Measured Solar Radiation and BATS-Estimated and Measured Reflected Shortwave Radiation, Surface Temperature, and Net Radiation for Each Site

Site	Description	Solar Radiation, W m^{-2}			Reflected Shortwave Radiation, W m^{-2}			Surface Temperature, W m^{-2}			Net Radiation, W m^{-2}		
		Mean	Mean Daily Min	Mean Daily Max	Mean	Mean Daily Min	Mean Daily Max	Mean	Mean Daily Min	Mean Daily Max	Mean	Mean Daily Min	Mean Daily Max
1	Measured	221.1	0.0	841.4	29.1	0.0	101.3	293.0	289.4	300.2	138.4	-84.7	705.5
	Forest				28.5	0.0	103.3	293.5	289.5	299.1	113.2	-103.5	666.8
	Deforested				43.3	0.0	156.9	291.8	283.3	306.2	102.7	-79.1	570.2
2	Measured	87.1	0.0	766.8	16.4	0.0	111.3	293.5	285.6	302.2	70.5	-49.0	686.9
	Forest				13.9	0.0	94.6	293.7	290.3	301.3	29.2	-83.8	626.3
	Deforested				21.4	0.0	145.3	291.5	285.0	309.4	29.6	-62.7	547.9
3	Measured	238.1	0.0	961.0	38.8	0.0	139.6	298.2	287.1	322.9	112.8	-66.6	650.8
	Forest				27.8	0.0	111.2	295.0	289.7	302.7	115.6	-101.6	728.9
	Deforested				42.4	0.0	169.2	292.9	283.4	311.0	106.8	-76.4	626.8
4	Measured	227.8	0.0	977.2	19.3	0.0	85.7	295.5	287.9	314.5	145.0	-53.7	791.3
	Forest				26.7	0.0	113.3	298.1	292.2	304.1	104.3	-100.5	759.7
	Deforested				40.6	0.0	172.2	296.0	287.1	312.9	96.9	-85.7	669.0
5	Measured	218.5	0.0	778.4	37.7	0.0	123.4	299.7	292.4	310.5	95.7	-65.1	544.1
	Forest				25.8	0.0	90.9	299.6	294.4	305.4	93.2	-105.4	574.6
	Deforested				39.5	0.0	139.4	298.3	288.7	312.7	83.0	-86.6	484.3
6	Measured	190.9	0.0	961.8	29.8	0.0	135.2	296.8	292.5	305.6	139.6	-62.2	809.5
	Forest				25.7	0.0	116.6	296.8	292.0	306.6	108.4	-90.8	796.7
	Deforested				39.4	0.0	178.8	296.4	287.5	315.1	96.5	-73.4	688.6
7	Measured	120.2	0.0	588.8	32.3	0.0	149.8	298.9	293.4	311.1	138.7	-51.3	780.5
	Forest				25.5	0.0	118.8	298.1	292.6	306.9	117.3	-81.9	821.6
	Deforested				39.0	0.0	181.6	296.9	288.0	315.4	104.8	-59.9	721.8

for the deforested than the forest simulation. Comparisons indicate that except for the most heavily disturbed sites, the deforested simulation overestimates the diurnal range of surface temperature. This finding is consistent with the fact that grassland represents the most extreme among the variety of land covers that replace tropical forest.

Net radiation is controlled by variations in solar radiation, reflected shortwave radiation, and surface temperature. Greater shortwave reflection and higher daytime surface temperature result in lower daytime net radiation for deforested surfaces; lower nighttime surface temperature reduces the magnitude of negative net radiation at night. Mean measured net radiation was higher than either simulation and appeared to be closely matched by the forest simulation (Figure 6) at all sites except harvested barley (site 3). The RMSE analysis (Table 12) confirms that for all sites except harvested barley, the forest simulation is closer to observations than the deforested. Even the lowest net radiation RMSE values, i.e., those for harvested barley versus the deforested simulation, 3-year secondary vegetation versus either simulation, and fallow rice paddy, 8-year and 25-year secondary vegetation versus the forest simulation, amount to errors of the order of a fifth to a third of mean measured net radiation.

Again, the excessively high albedo shift prevents the model from accurately portraying radiative exchange at most deforested sites during the day. The resulting underestimate of net radiation has implications for subsequent model estimates of sensible and latent heat flux.

Model-simulated soil moisture in surface and root zone layers are compared with TDR measurements at sites 1, 2, 6, 8, and 9 in Figures 7 and 8. Sites are arranged in the figures in order of time since most recent use. Because actual initial conditions at each site differed, model results are given in terms of soil moisture change. TDR measurements, which begin at various dates at different sites, are given as the change relative to both forest and deforested simulation values on the day TDR measurements started at each site. The root zone is defined in the model as the upper 1.5-m layer for the forest and the upper 1.0-m layer for the deforested case. TDR measurements are presented accordingly for comparison with each simulation.

Surface soil moisture (Figure 7) is reasonably well predicted by the forest simulation at all five TDR sites. RMSEs are lower for the forest simulation than the deforested for all sites (Table 12). For the three sites with measurements during the early part of the simulation (harvested corn, 8-year secondary vegetation, and exploited primary forest), the deforested simulation overestimates evaporative soil moisture loss during the rainless period from late January to early March. The deforested simulation also overestimates the magnitude of surface soil moisture increase after the start of rains. The tendency of the deforested simulation to overestimate soil evaporation indicates that the soil moisture observation sites had greater vegetative cover than is prescribed for grassland.

Root zone soil moisture change (Figure 8) measured at the harvested corn and exploited primary forest sites are both close to the forest simulation until the start of rains in late April. Measurements at the 8-year secondary vegetation site are reasonably well depicted by either simulation. At other sites, increases at the start of rains are

Table 12. Root Mean Square Error (RMSE) of Modeled Versus Measured Reflected Shortwave Radiation, Surface Temperature, Net Radiation, Surface Soil Moisture Change, and Root Zone Soil Moisture Change for Each Site

		Root Mean Square Error		
Climate Variable	Site	Model Forest	Model Deforested	N
Reflected shortwave, W m^{-2}	1	8.15	26.64	3846
	2	5.38	12.81	657
	3	19.74	14.22	1124
	4	13.96	37.73	702
	5	18.78	6.91	591
	6	8.23	17.17	2430
	7	11.62	13.30	1675
Surface temperature, K	1	1.29	5.62	4237
	2	1.62	4.15	649
	3	8.77	6.21	1112
	4	6.79	3.28	702
	5	3.08	2.72	591
	6	1.42	4.97	2753
	7	2.33	3.80	1675
Net radiation, W m^{-2}	1	33.62	69.53	4237
	2	45.04	52.12	657
	3	45.00	22.10	1124
	4	46.03	62.40	702
	5	32.23	33.24	570
	6	38.60	61.69	2753
	7	33.46	43.99	1675
Surface soil moisture, mm	1	6.38	13.06	21
	2	6.20	9.62	16
	6	5.44	8.39	8
	8	3.84	9.24	17
	9	2.69	6.80	16
Root zone soil moisture, mm	1	13.80	14.33	21
	2	44.31	20.76	16
	6	4.66	4.38	6
	8	35.75	17.08	17
	9	31.59	20.13	16

underestimated by both simulations. Root zone soil moisture RMSEs are lower for the deforested than forest simulations for all sites except 8-year secondary vegetation. Underestimation of root zone soil moisture increases following rains may be due, in part, to the use of low values for soil hydraulic conductivity (K_s) in both simulations. Measured K_s (Table 7) was higher at all sites than either the forested or the deforested parameter setting (Table 3) by as much as 2 orders of magnitude.

Summary and Conclusions

The BATS model was used in uncoupled mode to simulate forest cover and a deforested landscape, both defined as in recent GCM deforestation experiments. The model was forced by measurements of atmospheric variables during a 4-month period over a deforested area of mountainous northern Thailand. Measurements of reflected shortwave radiation, surface radiative temperature, net radiation, and soil moisture change in surface and root zone layers for a variety of deforested sites were compared with values predicted by the model for the forest and deforested cases. Comparisons of deforested simulation with measurements revealed (1) reflected shortwave radiation: deforested simulation exceeded measured values at all sites; (2) surface temperature: mean and diurnal range of observed values were close to those of the deforested simulation only for exposed soil; at the driest site (harvested barley), midday surface temperature exceeded that of the deforested simulation by nearly 12 K; at other sites, deforested simulation overestimated diurnal range; (3) net radiation: the mean for the deforested simulation underestimated measurements at all sites; the deforested simulation was relatively close to measured values at all sites during the night; mean diurnal range of the deforested simulation was lower than that measured at all sites; (4) surface soil moisture change: the deforested simulation overestimates evaporative soil moisture loss during the rainless period from late January to early March for the three sites with measurements during the period and overestimates soil moisture increase following the start of rains; (5) root-zone soil moisture change: the deforested simulation is close to measurements at the 8-year secondary vegetation site but underestimates increases at the start of rains at all other sites.

The results of comparisons lead to several conclusions regarding GCM simulations of the effects of deforestation on climate: (1) in terms of land surface-atmosphere interaction, most deforested land surfaces for which measurements were made in northern Thailand resemble simulated forest more closely than simulated grassland; (2) differences between measurements for deforested sites and values simulated in the deforested model run increase with time since abandonment; (3) secondary vegetation sites, 8 and 25 years after abandonment, were very similar in terms of land surface-atmosphere interaction to simulated forest; (4) daytime simulation of radiative exchange for a deforested surface is poor, presumably because of the excessively high albedo shift used to represent the effect of deforestation; (5) the relatively close correspondence between the advanced secondary forest measurements and the forest simulation suggests that misrepresentation of land surface-atmosphere interaction for deforested sites is associated with parameter specifications rather than the model itself.

The results presented here serve as a reminder that regardless of the quality of the model, simulations are only as good as the specification of parameter values and suggest strongly that subsequent GCM simulations of the climatic effects of tropical deforestation employ more realistic parameter settings to describe the deforested land surface. In particular, characteristics of the variety of land surfaces found in existing deforested areas should be considered in the prescription of postforest albedo, roughness length, soil hydrologic properties and other important land surface parameters. Recent land cover analyses as well as the constraints on the use of tropical land surfaces for agriculture suggest that secondary vegetation will remain an important replacement land cover in tropical deforested areas.

At the outset of the effort to use numerical simulation to predict effects of tropical deforestation on climate, *Henderson-Sellers and Gornitz* [1984] intentionally maximized the prescribed changes in land surface characteristics. The use of the "improverished grassland" scenario, however, is becoming accepted as a realistic depiction of the future state of presently forested areas of the tropics in

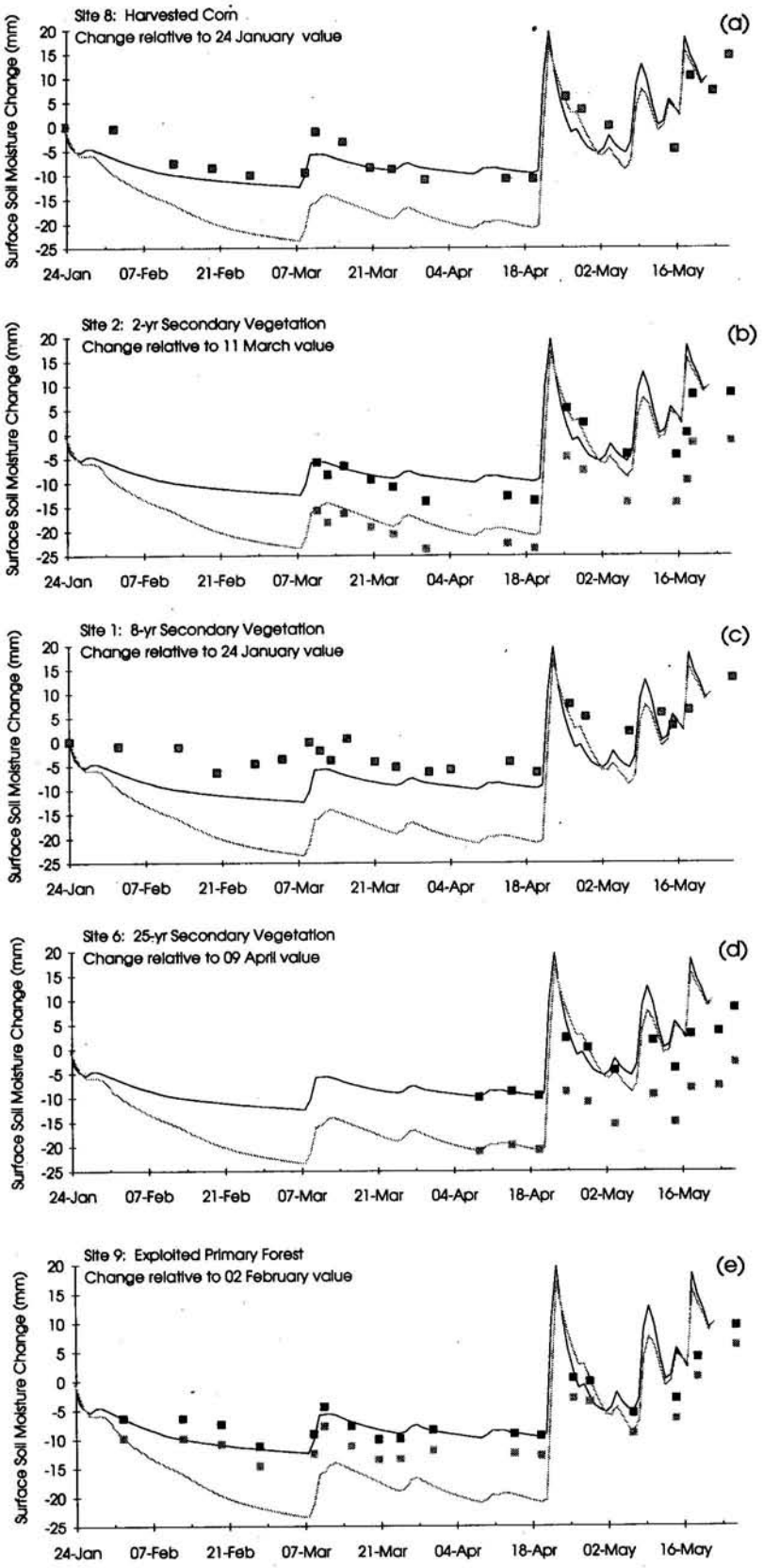

Figure 7. Change in surface layer (0 to 0.1 m) soil moisture simulated by BATS (lines) and measured using TDR (squares) at (a) harvested corn, (b) 2-year secondary vegetation, (c) 8-year secondary vegetation, (d) 25-year secondary vegetation, and (e) exploited primary forest. Forest (black lines) and deforested (grey lines) simulations, and measurements (grey squares with black border) are shown relative to the January 24 value. Measurements are shown relative to the simulated forest value on the first day of measurement (black squares) and simulated deforested value on the first day of measurement (grey squares) for sites where measurements began after January 24.

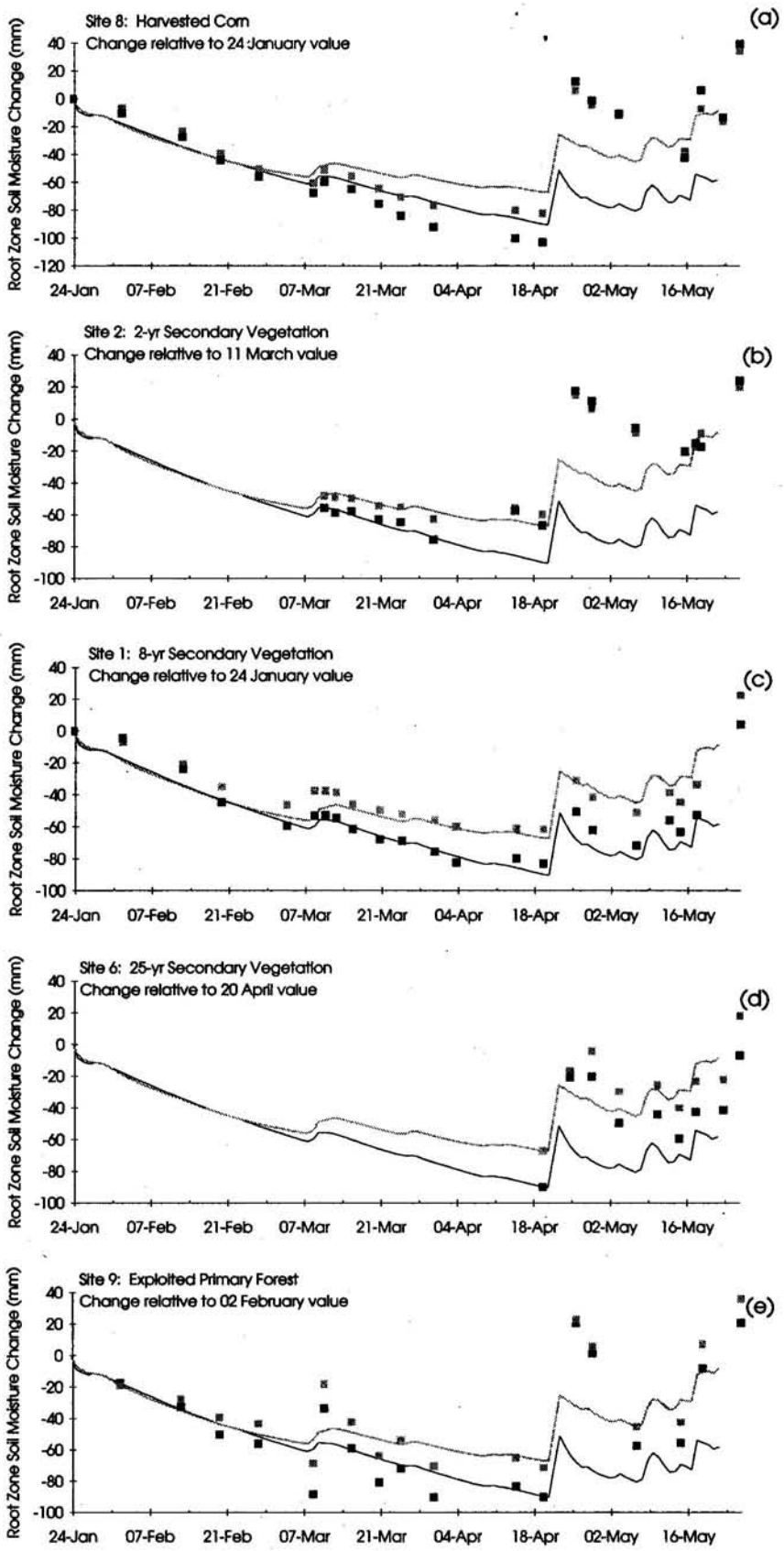

Figure 8. Change in root zone (0 to 1.5 m, forest; and 0 to 1 m, deforested) soil moisture simulated by BATS (lines) and measured using TDR (squares) at (a) harvested corn, (b) 2-year secondary vegetation, (c) 8-year secondary vegetation, (d) 25-year secondary vegetation, and (e) exploited primary forest. Forest (black lines) and deforested (grey lines) simulations are shown relative to the January 24 value. Measurements are shown for the upper 1.5 m layer relative to the simulated forest value on the first day of measurement (black squares) and for the upper 1 m layer relative to simulated deforested value on the first day of measurement (grey squares).

spite of much evidence to the contrary. Now that simulations with the extreme deforestation scenario are consistently predicting significant changes in the hydrologic cycle in the deforested regions, including large reductions in rainfall, the time may have come to run the models with more realistic parameter settings. However, development of a realistic deforestation scenario will depend on the availability of reliable characterizations of the physical properties of the various surfaces comprising the deforested landscape, and the land cover data from which realistic depictions of future deforested landscapes can be made.

Delineation of land cover at the global scale relies heavily on satellite remote sensing. Deforestation rates based on remotely sensed data may fail to provide information on the evolution of deforested surfaces. Land cover change, particularly in the tropics, has been shown to be a dynamic process involving loss of forest partly offset by rapid regrowth of secondary vegetation [*Turner et al.*, 1993]. Our study suggests that secondary vegetation increasingly (with time since abandonment) resembles the original forest cover and therefore that the climatic impacts of deforestation may be less than that implied by the rate of tree felling. Assessment of current levels and rates of deforestation, which must ultimately form the basis of future deforestation scenarios, has been confounded by the difficulty in distinguishing secondary vegetation from forest in satellite data. Recent analyses, such as those of *Moran et al.* [1994] and *Watrin* [1994], however, demonstrate the ability to identify secondary vegetation at different growth stages and point to improved deforestation assessments.

Changes in energy and mass fluxes in deforested areas that have been abandoned for a number of years are likely to be much smaller than the large changes found by investigators such as *Xue et al.* [1996] for actively used deforested sites. Our results suggest that while significant regional climate change is a probable consequence of large-scale tropical deforestation, the effects may be less severe than those predicted by recent GCM experiments if future deforestation continues to result in a diverse pattern of replacement cover, such as that found in currently deforested areas. These results are in no way intended to encourage current practices leading to rapid forest loss in the tropics. The continuing effects of deforestation on atmospheric chemistry, loss of plant biodiversity and animal habitats, and the destruction of the cultures of forest-dwelling people will remain critical issues undiminished by any future reassessments of direct climate effects.

Acknowledgements. The research reported here was initiated and carried out with the support and cooperation of numerous individuals associated with the Sam-Mun Highland Development Project; Multiple Cropping Centre, the Geography Department, and the Biology Department at Chiang Mai University; and the Program on Environment at the East-West Center in Honolulu. We are most grateful to Samer Limchoowong (Sam-Mun Highland Development Project), Methi Ekasingh (Multiple Cropping Centre), Sanay Yarnasarn and Pichayet Onibutr (Geography Department, Chiang Mai), F. Maxwell (Biology Department, Chiang Mai), and Jefferson Fox (Program on Environment). We are also deeply indebted to the people of Pang Khum who gave generously of their knowledge of the land and allowed us to use their land for our measurements. We are especially thankful for the kindness of the Paluk Lamer family who provided accommodations in Pang Khum as well as advice and assistance at every stage of the field research. Financial support for the field study was provided by the Committee for Research and Exploration, National Geographic Society (grant number 4923-92) and by a University of Hawaii—East-West Center Collaborative Research Grant. We are grateful to Zong-Liang Yang and other members of the BATS Core Group at the University of Arizona for providing the BATS code and giving advice in the use of the model.

References

Andre, J.C., J.P. Goutorbe, and A. Perrier, HAPEX-MOBILHY: A hydrologic atmospheric experiment for the study of water budget and evaporation flux at the climatic scale, *Bull. Am. Meteorol. Soc., 67*, 138-144, 1986.

Betts, A.K., J.H. Ball, A.C.M. Belijarrs, Comparison between the land surface response of the ECMWF model and the FIFE-1987 data, *Q.J.R. Meteorol. Soc., 119*, 975-1001, 1993.

Betts, A.K., J.H. Ball, A.C.M. Beljaars, M.J. Miller, and P.A Viterbo, The land-surface interaction: a review based on observational and global modeling perspectives, *J. Geophys. Res., 101*, 7209-7225, 1996.

Chen, F., K. Mitchell, J. Schaake, Y. Xue, H.-L. Pan, V. Koren, Q.Y. Duan, M. Ek, and A.K. Betts, Modeling of landsurface evaporation by four schemes and comparison with FIFE observations, *J. Geophys. Res., 101, 7251-7268, 1996.*

Culf, A.D., G. Fisch, and M.G. Hodnett, The albedo of Amazonian forest and ranchland, *J. Clim., 8*, 1544-1554, 1995.

Dalton, F.N., Development of time-domain reflectometry for measuring soil water content and bulk soil electrical conductivity, in *Advances in measurement of soil properties: Bringing theory into practice*, edited by G.C. Topp, W.D. Reynolds, and R.E. Green, pp. 143-167, *Spec. Publ. 30*, Soil Sci. Soc. Am., Madison, Wis., 1992.

Dickinson, R.E., Implications of tropical deforestation for climate: A comparison of model and observational descriptions of surface energy and hydrological balance, *Philosophical Trans. R. Soc. London B*, 324, 423-431, 1989.

Dickinson, R.E., and P.J. Kennedy, Impacts on regional climate of Amazon deforestation, *Geophys. Res. Lett., 19*, 1947-1950, 1992.

Dickinson, R.E., and A. Henderson-Sellers, Modelling tropical deforestation: A study of GCM land-surface parameterizations, *Q.J.R. Meteorol. Soc., 114*, 439-462, 1988.

Dickinson, R.E., A. Henderson-Sellers, P.J. Kennedy, and M.F. Wilson, Biosphere-atmosphere transfer scheme (BATS) for the NCAR community climate model, *Tech Note/TN-275+STR*, Nat. Cent. for Atmos. Res., Boulder, Colo., 1986.

Dickinson, R.E., A. Henderson-Sellers, and P.J. Kennedy, Biosphere-atmosphere transfer scheme (BATS) version 1e as coupled to the NCAR community climate model, *Tech Note/TN-387+STR*, Nat. Cen. for Atmos. Res., Boulder, Colo., 1993.

Dirmeyer, P.A., and J. Shukla, Albedo as a modulator of climate response to tropical deforestation, *J. Geophys. Res., 99*, 20,863-20,878, 1994.

Erbs, D.G., S.A. Klein, and J.A. Duffie, Estimation of the diffuse radiation fraction for hourly, daily and monthly-average global radiation, *Sol. Energy, 28*, 293-304, 1982.

Food and Agriculture Organization (FAO), United Nations, *1989 Production Yearbook*, Rome, Italy, 1990.

Fox, J., R. Kanter, S. Yarnasarn, M. Ekasingh, and R. Jones, Farmer decision making and spatial variables in Northern Thailand, *Environ. Manage., 18*, 391-399, 1994.

Fox, J., J. Krummel, S. Yarnasarn, M. Ekasingh, and N. Podger, Land use and landscape dynamics in Northern Thailand: Assessing change in three upland watersheds, *Ambio 24*, 328-334, 1995.

Giambelluca, T.W., Tropical land cover change: Characterizing the post-forest land surface, in *Climate Change: Developing Southern Hemisphere Perspectives*, edited by T.W.

Giambelluca and A. Henderson-Sellers, pp. 293-318, John Wiley, Chichester, U.K., 1996.

Hansen, P.K., An account of the forest in a watershed area in northern Thailand, Dep. of Econ. and Nat. Resources, Unit of Forestry, Royal Veterinary and Agric. Univ., Copenhagen, 1992.

Henderson-Sellers, A., Land surface process models discussed in interdisciplinary forum. *Eos Trans. AGU, 76*, 369-379, 1995.

Henderson-Sellers, A., and R.E. Dickinson. Intercomparison of land surface parameterisations launched. *Eos Trans. AGU, 73*, 195-196, 1992.

Henderson-Sellers, A., and V. Gornitz, Possible climatic impacts of land cover transformations, with particular emphasis on tropical deforestation, *Clim. Change, 6*, 231-257, 1984.

Henderson-Sellers, A., R.E. Dickinson, T.B. Durbridge, P.J. Kennedy, K. McGuffie, and A.J. Pitman, Tropical deforestation: Modeling local- to regional-scale climate change, *J. Geophys. Res., 98*, 7289-7315, 1993a.

Henderson-Sellers, A., Z.-L. Yang, and R.E. Dickinson, The project for intercomparison of land-surface parameterization schemes, *Bull. Am. Meteorol. Soc., 74*, 1335-1349, 1993b.

Henderson-Sellers, A., A.J Pitman, P.K. Love, P. Irannejad, and T.H. Chen, The Project for Intercomparison of Land Surface Parameterization Schemes (PILPS): Phases 2 and 3, *Bull. Am. Meteorol. Soc., 76*, 489-503, 1995.

Henderson-Sellers, A., H. Zhang, and W. Howe, Human and physical aspects of tropical deforestation, in *Climate Change: Developing Southern Hemisphere Perspectives*, edited by T.W. Giambelluca and A. Henderson-Sellers, pp. 259-292, John Wiley, Chichester, U.K., 1996.

Houghton, R.A, The worldwide extent of land-use change, *BioSci., 44*, 305-313, 1994.

Jacquemin, B., and J. Noilhan, Sensitivity study and validation of a land surface parameterization using the HAPEX-MOBILHY data set, *Boundary-Layer Meteorol., 52*, 93-134, 1990.

Love, P.K., and A. Henderson-Sellers, Land surface climatologies of AMIP-PILPS models and identification of regions for investigation, *Program for Climate Model Diagnosis and Intercomparison (PCMDI) Rep.* 83 pp., 1994.

Mahfouf, J-F., A numerical simulation of the surface water budget during HAPEX-MOBILHY. *Boundary-Layer Meteorol., 53*, 201-222, 1990.

Mahfouf, J.-F., and B. Jacquemin, A study of rainfall interception using a land surface parameterization for mesoscale meteorological models, *J. Appl Meteorol., 28*, 1282-1302, 1989.

McGuffie, K., A. Henderson-Sellers, H. Zhang, T.B. Durbridge, and A.J. Pitman, Global sensitivity to tropical deforestation, *Global Planet. Change, 10*, 97-128, 1995.

Monna, W.A.A., and J.G. Van Der Vliet, Facilities for research and weather observations on the 213-m tower at Cabauw and at remote locations, *Sci. Rep. WR-87-5*, 27 pp., KNMI, De Bilt, Netherlands, 1987.

Moran, E.F., E. Brondizio, P. Mausel, and Y. Wu, Integrating Amazonian vegetation, land-use, and satellite data, *BioSci., 44*, 329-338, 1994.

Myers, N., Tropical forests: Present status and future outlook, *Clim. Change, 19*, 3-32, 1991.

Noilhan, J., and S. Planton, A simple parameterization of land surface processes for meteorological models, *Mon. Weather Rev., 117*, 536-549, 1989.

Pitman, A.J., and A. Henderson-Sellers, Simulating the diurnal temperature range: Results from phase 1(a) of the Project for Intercomparison of Land Surface Parameterisation Schemes (PILPS), *Atmos. Res., 37*, 229-245, 1995.

Pitman, A.J., et al., Project for Intercomparison of Land-Surface Parameterization Schemes (PILPS): Results from off-line simulations (phase 1a), *Publ. Ser. 7*, Int. GEWEX Proj. Off., Washington, D.C. 1993.

Polcher, J., and K. Laval, The impact of African and Amazonian deforestation on tropical climate, *J. Hydrol., 155*, 389-405, 1994.

Richards, J.F., and E.P. Flint, *Historic Land Use and Carbon Estimate for South and Southeast Asia: 1880-1980*, edited by R.C. Daniels, *Publ. 4174*, Carbon Dioxide Inf. Anal. Cent., Oak Ridge Nat. Lab., Environ. Sci. Div., 1994.

Sellers, P.J., and J.L. Dorman, Testing the simple biosphere model (SiB) using point micrometeorological and biophysical data, *J. Clim. Appl. Meteorol., 26*, 622-651, 1987.

Sellers, P.J., Y. Mintz, Y.C. Sud, and A. Dalcher, A simple biosphere model (SiB) for use within general circulation models, *J. Atmos. Sci., 43*, 505-531, 1986.

Sellers, P.J., F.G. Hall, G. Asrar, D.E. Strebel, and R.E. Murphy, The First ISLSCP Field Experiment (FIFE), *Bull. Am. Meteorol. Soc., 69*, 22-27, 1988.

Sellers, P.J., W.J. Shuttleworth, J.L. Dorman, A. Dalcher, and J.M. Roberts, Calibrating the simple biosphere model for Amazonian tropical forest using field and remote sensing data, I, Average calibration with field data, *J. Appl. Meteorol., 28*, 727-759, 1989.

Shuttleworth, W.J., Evaporation from Amazonian rainforest, *Proc. R. Soc. London B, 233*, 321-346, 1988.

Shuttleworth, W.J., et al., Eddy correlation of energy partition for Amazonian forest, *Q.J.R. Meteorol. Soc., 110*, 1143-1162, 1984a.

Shuttleworth, W.J., et al., Observations of radiation exchange above and below Amazonian forest, *Q.J.R. Meteorol. Soc. 110*, 1163-1169. 1984b.

Shuttleworth, W.J., J.H.C. Gash, J.M. Roberts, C.A. Nobre, L.C.B. Molion, and M.N.G. Ribeiro, Post-deforestation Amazonian climate: Anglo-Brazilian research to improve prediction. *J. Hydrol., 129*, 71-85, 1991.

Sud, Y.C., G.K. Walker, J.-H. Kim, G.E. Liston, P.J. Sellers, and K.-M. Lau, Biogeophysical effects of a tropical deforestaion scenario: a GCM simulation study, *J. Clim.*, in press, 1996.

Turner, B.L., R.H. Moss, and D.L. Skole. Relating land use and global land-cover change: A proposal for an IGBP-HDP core project, International geosphere-biosphere programme: a study of global change and the human dimensions of global envrionmental change, *IGBP rep. 24*, International Geophysical-Biosphere Programme, Stockholm, 1993.

Watrin, O.D.S., Análise da dinâmica na paisagem agrícola da Amazônia oriental: Abordagem integrando técnicas de processamento digital de imagens e sistemas de informação geográfica, Ph.D. dissertation, Ministério da Ciência e Tecnol. Inst. Nac. de Pesquisas Espaciais, São José dos Campos, Brazil, 1994.

Wright, I.R., J.H.C. Gash, H.R. Da Rocha, W.J. Shuttleworth, C.A. Nobre, G.T. Maitelli, C.A.G.P. Zamparoni, and P.R.A. Carvalho, Dry season micrometeorology of central Amazonian ranchland, *Q.J.R. Meteorol. Soc., 188*, 1083-1099, 1992.

Wright, I.R., C.A. Nobre, J. Tomasella, H.R. da Rocha, J.M. Roberts, E. Vertamatti, A.D. Culf, R.C. Alvalá, M.G. Hodnett, and V. Ubarana, Towards a GCM surface parameterization for Amazonia, in *Amazonian Deforestation and Climate*, edited by J.H.C. Gash, C.A. Nobre, J.M. Roberts, and R.L. Victoria, pp. 474-504, John Wiley, 1996.

Xue, Y., H.G. Bastable, P.A. Dirmeyer, and P.J. Sellers, Sensitivity of simulated surface fluxes to changes in land surface parameterizations—A study using ABRACOS data, *J. of Appl. Meteorol.*, 1996.

T.W. Giambelluca, T.P. Menard, M.A. Nullet, L.T. Tran, and A.D. Ziegler, Department of Geography, University of Hawaii at Manoa, 2424 Maile Way #445, Honolulu, HI 96822. (email: tom@climate.soc.hawaii.edu; trae@climate.soc.hawaii.edu; mike@climate.soc.hawaii.edu, liem@climate.soc.hawaii.edu; alan@climate.soc.hawaii.edu)

(Received November 15, 1995; revised May 30, 1996; accepted June 4, 1996.)